

## Time-frequency-space localization of epileptic EEG oscillations

**Artur Matysiak<sup>1</sup>, Piotr J. Durka<sup>1</sup>, Eduardo Martinez Montes<sup>2</sup>,  
Marek Barwiński<sup>3,4</sup>, Piotr Zwoliński<sup>5</sup>, Marcin Roszkowski<sup>5</sup>,  
and Katarzyna J. Blinowska<sup>1</sup>**

<sup>1</sup>Department of Biomedical Physics, Institute of Experimental Physics,  
Warsaw University, 69 Hoża St., 00-681 Warsaw, Poland; <sup>2</sup>Cuban  
Neuroscience Center, Ave 25 #15202 Esquina 158, Cubanacan, Playa, 11600  
Havana, Cuba; <sup>3</sup>Institute of Neuroinformatics, Ruhr-University,  
Universitätsstrasse St 160, 44780 Bochum, Germany; <sup>4</sup>International Graduate  
School of Neuroscience, Ruhr-University, Universitätsstrasse St. 150, 44780  
Bochum, Germany; <sup>5</sup>Department of Neurosurgery, Memorial Child Health  
Institute, 20 Dzieci Polskich St., 04-736 Warsaw, Poland

**Abstract.** This paper presents a hybrid method for localization of oscillatory EEG activity. It consists of two steps: multichannel matching pursuit with complex Gabor dictionary, and LORETA inverse solution. Proposed algorithm was successfully applied to the localization of epileptogenic EEG in a single patient.

The correspondence should be  
addressed to A. Matysiak,  
Email: [amatys@fuw.edu.pl](mailto:amatys@fuw.edu.pl)

**Key words:** EEG, multichannel matching pursuit, inverse solution,  
LORETA, epilepsy

## INTRODUCTION

The essential task for an epileptologist is to localize the epileptic zone. Possible non-invasive and invasive EEG-derivate determination of electric pacemaker is then – in eligible cases – followed by resection of delineated zone. Any possibly reliable mathematical aids are thus very demandable to help in localizing procedures.

In line with these clinical and research needs, there is an increasing interest in the characterization – in time, frequency and space – of structures or activities from the electroencephalographic (EEG) traces (Konig et al. 2001, Miwakeichi et al. 2004). Despite some attempts in using truly multidimensional decomposition methods (Miwakeichi et al. 2004), still the most popular approach has been the combination of methods for bilinear decomposition in two of these dimensions and some other estimation procedure for characterization of the third dimension. Following the general idea proposed by Durka and coauthors (2005), in this study we implement a method based upon two following steps: (i) multichannel adaptive time-frequency parameterization of the EEG time series; (ii) EEG inverse solution.

For the first step we use a multichannel matching pursuit (mmp) (Gribonval 2003) applied to the (analytic) EEG signal, using a dictionary of complex Gabor atoms. The algorithm provides a set of complex weights for each electrode, which define a spatial distribution (topography) on the scalp for given complex atom. This topography is then subjected to source localization (second step), with the use of Low Resolution Electromagnetic Tomography (LORETA) (Pascual-Marqui et al. 1994). This instantaneous inverse solution provides a maximum smoothness for the distribution of primary current density (PCD) inside the brain. Performance of this hybrid algorithm is presented on an epileptic EEG signal from a single patient. Complex Gabor atoms were extracted from the mmp parameterization of the signal, based upon their time-frequency properties corresponding to epileptic oscillatory activity.

Different time-frequency-space localization procedures include e.g., the classical method, relying on spectral integrals (it was compared to the adaptive time-frequency preprocessing by Martinez-Montes and coauthors (2005)). Other method, presented by Geva (1998), uses an mmp algorithm similar to the imple-

mentation used in this work, but solves the inverse problem by a linear exhaustive search with sources constrained to a particular grid of the brain and supposed to be single or symmetrical pairs of current dipoles. Another kind of inverse solution, called Source Spectra Imaging (SSI), was used for finding the spectra of the current density distribution after obtaining topographic signatures from three-dimensional decomposition of the spontaneous EEG time-varying spectrum (Martinez-Montes et al. 2004, Miwakeichi et al. 2004).

There were also previous attempts to localize sources of epileptic activity. The method presented by Holmes and coauthors (2004) used LORETA inverse solution for spike components of each spike-wave burst. In this case use of LORETA needs heavy statistical postprocessing. Other method, presented by Worrell and coauthors (2000), used phase-encoded frequency spectral analysis (PEFSA) for characterizing time-frequency structures. It has similar properties as the mmp with complex Gabor dictionaries, but the inverse solution LORETA was done for real weights obtained by projection of the complex weights onto the best-fit line, and in this work we perform LORETA inverse solution for complex weights.

## METHODS

### Multichannel matching pursuit (mmp)

In this study, multichannel matching pursuit (mmp) procedure is applied to the analytic (Bracewell 1986) signal  $\mathbf{S}^H_{N \times N_t} = \mathbf{S}_{N \times N_t} - iH(\mathbf{S}_{N \times N_t})$ , where  $H$  denotes the Hilbert transform performed independently for every channel, and  $\mathbf{S}_{N \times N_t}$  is the original, real-valued EEG. Mmp decomposes this signal into a linear sum of functions (time-frequency atoms), chosen adaptively from a redundant set called dictionary  $\mathbf{D}$ . In the following we shall denote these atoms as MD Gabors, that is complex multidimensional Gabor functions. MD Gabor is a matrix  $\mathbf{M}_{N \times N_t}^\gamma$  equal to the outer product of transposed vector of complex weights for each channel  $\mathbf{W}_{N \times 1}^\gamma$  and normalized 1D complex Gabor function  $G_{1 \times N_t}^\gamma$  (abbrev: 1D Gabor).

$$\mathbf{M}_{N \times N_t}^\gamma = \mathbf{W}_{N \times 1}^\gamma \mathbf{G}_{1 \times N_t}^\gamma \quad (1)$$

1D Gabor  $G^\gamma$  can be characterized by three parameters: time position  $u$ , frequency position  $\omega$  and duration  $\sigma$ ,

and the index  $\gamma = \{u, \omega, \sigma\}$  represents the set of those three parameters.

$$G_{1 \times Nt}^{\gamma} = \frac{2^{1/4}}{\sqrt{\pi}} e^{\frac{\pi(t-u)^2}{\sigma^2} + i\omega t} \quad (2)$$

The time is discrete  $t = [\delta t \dots Nt \delta t]$ . 1D Gabor is normalized i.e.,  $\|G^{\gamma}\|^2 = 1$ . A complex weight  $w_e^{\gamma}$  is a scalar product between 1D Gabor  $G_{1 \times Nt}^{\gamma}$  and the signal in  $e^{\text{th}}$  channel  $\mathbf{S}_{1 \times Nt}^{eH}$ .

$$w_e^{\gamma} = \langle S^{eH}, G^{\gamma} \rangle = \sum_{t=1}^{Nt} s_t^{eH} g_t^{\gamma*} \quad (3)$$

Finally, the mmp is an iterative procedure, working on the residua  $R^{a+1} \mathbf{S}_{Ne \times Nt}^H$ , left from the signal after subtracting results of the previous  $a$  iterations. The signal itself is treated as the  $O^{\text{th}}$  residuum  $R^0 \mathbf{S}_{Ne \times Nt}^H$ . In each step, the algorithm finds an MD Gabor  $\mathbf{M}_{Ne \times Nt}^{\gamma}$ , fitting best the residuum:

$$\begin{cases} R^0 \mathbf{S}_{Ne \times Nt}^H &= \mathbf{S}_{Ne \times Nt}^H \\ \mathbf{M}_{Ne \times Nt}^a &= \arg \max_{\mathbf{M}^{\gamma} \in \mathbf{D}} \sum_{e=1}^{Ne} |\langle R^a \mathbf{S}_{Ne \times Nt}^{eH}, G_{1 \times Nt}^{\gamma} \rangle|^2 \\ R^{a+1} \mathbf{S}_{Ne \times Nt}^H &= R^a \mathbf{S}_{Ne \times Nt}^H - \mathbf{M}_{Ne \times Nt}^a \end{cases} \quad (4)$$

Linear multichannel decomposition obtained by mmp in matrix notation reads:

$$\mathbf{S}_{Ne \times Nt}^H = \mathbf{W}_{NaxNe}^T \mathbf{G}_{NaxNt} + R^{Na+1} \mathbf{S}_{Ne \times Nt}^H \quad (5)$$

The main difference between this implementation and the one presented in Durka and coauthors (2005) is that complex atom is now parameterized by only three parameters (time, frequency and duration), and the phase – possibly different in different channels – is contained in the complex weights.

The other difference is that the method presented by Durka and coauthors (2005) lacks exponential convergence properties presented by Mallat and Zhang (1993) and Gribonval (2003). On the other hand, it decays reasonably fast for multichannel EEG signal referenced to the linked ears or some other distant electrode, since in such references multichannel EEG signal tends to be composed of time-frequency structures with similar phases in different channels (Fig. 1). Also, numerical complexity of the algorithm proposed by Durka and coauthors (2005) is lower by a factor equal

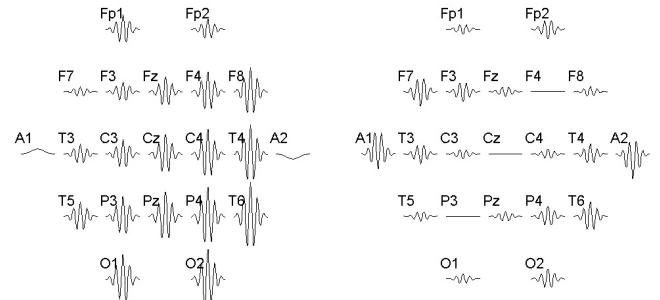


Fig. 1. Heuristic example of a possible EEG waveform, referenced to linked ears (left panel) and an electrode placed on the top of the skull (Cz, right panel). We observe that Cz reference introduces frequency structures in opposite phases in derivations from left/frontal and right/parietal locations.

to number of channels, compared to mmp presented by Gribonval (2003). In this study we use a structured redundant dictionary, that is with given time shift and frequency shift between consecutive Gabor atoms. Time width of all Gabor atoms in the dictionary was constant. The time shift and frequency shift were set to not exceed the value implied by the uncertainty principle.

#### Low resolution electromagnetic tomography (LORETA)

The standard time-domain EEG forward solution linearly relates scalp multichannel EEG time series  $\mathbf{S}_{Ne \times Nt}$  and the primary current density (PCD) time series  $\mathbf{J}_{3Nv \times Nt}$ . This relation can be written for  $\mathbf{S}^H$  and  $\mathbf{J}^H = \mathbf{J} - iH(\mathbf{J})$

$$\mathbf{S}_{Ne \times Nt}^H = \mathbf{K}_{Ne \times 3Nv} \mathbf{J}_{3Nv \times Nt}^H + \mathbf{E}_{Ne \times Nt}^H \quad (6)$$

where the rows of matrix  $\mathbf{J}^H$  correspond to thrice the number of voxel elements  $3Nv$ , corresponding to the  $x$ ,  $y$  and  $z$  components of the PCD vector in each voxel of a grid defined inside the brain, and columns correspond to time samples. The real matrix  $\mathbf{K}$ , linking the current density with the measurements, is called the lead field matrix and does not depend on time and frequency. It can be calculated by applying Maxwell's equations to a particular head model (Riera and Fuentes 1997). The matrix  $\mathbf{E}$  is an additive random element representing unmodeled effects such as the observation noise.

The EEG inverse problem is defined as the estimation of current density time series  $\mathbf{J}^H$  from EEG time series  $\mathbf{S}^H$  independently for every time point. Mathematically, it is an ill-conditioned (sensitive to noise) and ill-posed problem (non-uniqueness), so additional constraints are required for finding the so-called “inverse solution”.

There are several approaches for mathematically solving the problem from Eq. 6. The use of Tikhonov regularization (Tikhonov and Arsenin 1977) and a Bayesian approach (Trujillo-Barreto et al. 2004) have been the most popular. Furthermore, different constraints and prior information about the solution can lead to a different inverse solution. Yet, there is not a “best” inverse solution. However, due to its simple implementation, low computational cost and generally good properties in terms of localization error (Pascual-Marqui et al. 1994), LORETA is the most popular among the distributed inverse solutions.

LORETA assumes that PCD values in neighboring voxels must be similar based on the usually higher inter-connectivity of near neurons. This implies the choice of the smoothest distribution of the PCD inside the brain. On the other hand, LORETA does not assume any dependency between different time points, so it is an instantaneous inverse solution.

With the approach used here, we assume that the PCD follows the dynamics of the EEG, since the lead field only affects the spatial dimension. Then, the topographies, defined by the mmp algorithm as corresponding to EEG structures with determined time-frequency properties, can be used as the input of instantaneous inverse solution. This can be seen in another way by comparing Eq. 5 and 6 and establishing the relation between topographies  $\mathbf{W}$  and the PCD signature  $\mathbf{J}'$  for corresponding MD Gabors.

$$\mathbf{W}_{NexNa}^H = \mathbf{K}_{Nex3Nv} \mathbf{J}_{3Nv \times Nt}^H + \mathbf{E}_{NexNt}^H \quad (7)$$

As the input for Eq. 7 consist of complex coefficients, the PCD will also be complex. However, given the properties of the Hilbert transform (Bracewell 1986), the real part of this magnitude will be the real electric current defining localization of the sources of the time-frequency structures represented by MD Gabor.

### Experimental data

We present a case of 7 year-old patient, M.K., female, suffering from epilepsy since 3 years. Her

seizures started with unilateral simple motor seizures (IA class of the ILAE classification) involving upper part of face (periocular muscles, twitches of eyes) and upper extremity (also twitches, mostly proximal arm). She developed also partial complex fits after some time, seizures soon occurred in clusters, presenting form of Kojevnikov epilepsy (epilepsia partialis continua) lasting for weeks, sometimes months. Various antiepileptic drugs (AED) were not effective, she developed resistance to all conventional and newer AED very soon.

In the following MRI scans we have found slowly progressing characteristic signal of inflammatory process starting within periinsular region of left hemisphere, typical (considering clinical picture) for Rasmussen syndrome (RS), which was the final diagnosis. EEG was always abnormal – however, the picture showed mild generalized pathology (slow waves) of background activity, and occasional ictal discharges of spikes and/or sharp waves in left hemisphere, mostly in centro-frontal region. She has had a lot of AED changes (with no effect at all), she was operated 3 times: first operation was an anterior callosotomy (tractotomy resection of the 2/3 anterior part of the corpus callosum), second was the implantation of NCP-102 vagal nerve neurostimulator, which was set to stimulate intermittently cervical portion of vagal nerve (VNS therapy, used in epilepsy treatment since 1997). Both operation failed, we had not achieved any seizure reduction. Typical surgical solution in such cases is hemispherectomy (total disconnection of the whole hemisphere – in this case left), however the procedure is very brutal, resulting of the contralateral hemiplegia, and in this case (left, dominant hemisphere) loss of speech. All those functions were not significantly disturbed, despite some mild Todd paresis after series of seizures. Girl also had very mild mental deterioration, which is typical in RS.

Therefore we decided to make selective resection (third operation) EcoG guided. After wide opening of the left hemisphere skull bone in modification of Yassargil mode we have performed the first ECoG which showed very frequent and marked discharges of spikes and spike-wave complexes within the frontal region (mostly middle and upper frontal gyrus), with spread of discharges to temporal lobe, parietal lobe (postcentral gyrus and even more rostral); after inspection of the temporal lobe we have also found some discharges from deep meso-limbic structures. We decided to resect the 3–4 cm of the temporal lobe (from the tip) with resection of deep structures, as well as the multi-

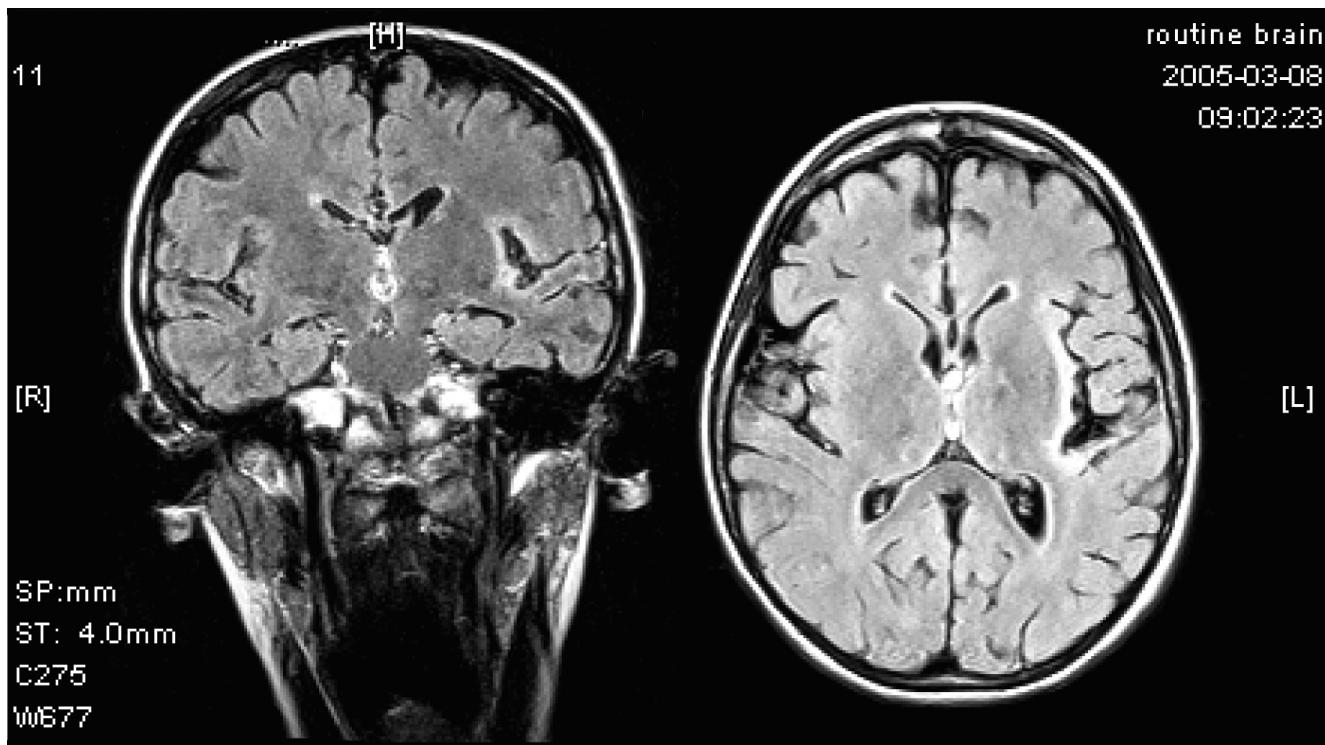


Fig. 2. MRI picture of the perinsular focal abnormality.

focal MST (Multifocal Subpial Transsections) sections of those regions of the hemisphere which shows discharges after the resection. We have ended the operation with almost silent trace of the EEG curve in ECoG. After the operation the girl still has some twitches of the upper part of the face, however seizures are mild and shorter. She does not experience cluster seizures or status epilepticus.

We assume that progressing character of the RS may come to a stage that hemispherectomy may be the only possible treatment, however – some cases of RS show no such progress.

#### Software

The mmp implementation uses analytic formula for inner product computations and FFT. The LORETA implementation was developed at Cuban Neuroscience Center and uses three-spherical head model and lead field as defined by Riera and Fuentes (1997).

Both mmp and LORETA used in this study were written in Matlab. They can be downloaded from the EEG.pl portal (<http://eeg.pl>, Section "software"). As the inverse solution visualization tool we used BetViewer developed at Cuban Neuroscience Center.

## RESULTS

The two-step procedure described in Methods section was applied to EEG signal recorded during epileptic attack of a patient described in Experimental data section. The epoch length was 8 s and sampling frequency was 256 Hz. The signal was digitally filtered with band pass Butterworth filter (between 1.6 Hz and 40 Hz) in forward and reverse directions. Then it was referenced to the average reference. The redundant dictionary **D** used for mmp decomposition consisted of shifted – in time and frequency – versions of 1D Gabor with one scale  $s=0.25$  s. Time shift was set as  $\Delta t=0.125$  s, and frequency shift  $\Delta f=0.25$  Hz.

Inverse solution was found with a version of LORETA algorithm implemented by Cuban Neuroscience Center. This implementation of LORETA is based upon singular value decomposition of the electric lead field for three homogenous concentric spheres model (Riera and Fuentes 1997), previously standardized by the discrete Laplacian operator. The equation for the solution stems from the minimization of the classical LORETA functional and the optimal regularization parameter is found by generalized

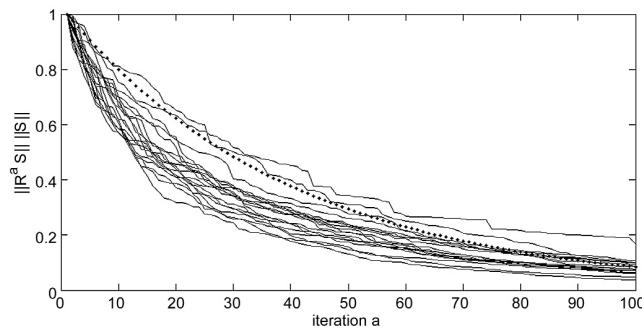


Fig. 3. Signal residuum norm decay for all channels (solid lines) and decay exponential function defined (dotted).

cross-validation technique, although it can be easily modified to maximize any other criteria, such as Akaike Information Criteria, Bayesian Information Criteria, and others.

Figure 3 presents decay of signal residuum's energy for all channels and the plot of a decay exponential function, defined as  $EXP(a) = \exp(-a/\text{factor})$ , where *factor* is chosen such as  $EXP(Na) = \|R^a S\|/\|S\|$ . It can be observed that residua decay faster than the corresponding exponential decay function for all but two channels above 50 iterations.

Top panel of Fig. 4 presents the considered EEG signal and a real part of the signal reconstructed from time-frequency atoms (MD Gabors) that were chosen as the epileptic ones. Middle panel presents schematic spatio-time-frequency map obtained for chosen atoms i.e., topographies of absolute values of complex weights are plotted in the corresponding points in the time-frequency plane for every chosen atom. Lower panel 4 presents schematic complex topographies for 8 time-frequency atoms, that is besides topography for given time-frequency atom (as in the middle plot) it shows also phases of complex weights as normalized vectors hooked in the middle of given topography area.

Resulting localization of the generators of chosen time-frequency structures are presented on Fig. 5. Norms of PCD vectors for these structures exhibit consistent activity in the middle and upper frontal gyrus part of the brain. It can be also seen that the PCD vectors flow parallel to the scalp between typical positions of electrode F3 and T5 (Fig. 5). This can be also concluded from the complex topography map of given time-frequency structure (lower panel of Fig. 3) – activity in electrodes F3 and T5 are high but in nearly opposite phases.

## DISCUSSION

In described case, patient was operated – she had temporal lobectomy complemented by a multiple subpial transsection (MST) in Morell mode (multiple cuts of the grey matter of hemisphere, disconnecting conjuctions between neurons, done under pia mater). The resection was delineated by electrocorticography (ECoG) which showed broad area of epileptic discharges, mainly in temporal/frontal border, temporal lobe and some parts of parietal lobe. The area of discharges corresponded to the one delineated from the scalp EEG using the procedure presented in this paper. Due to the fact, that some areas of discharges were placed in eloquent zones of brain, only partial lobectomy could be done (Spencer mode topectomy of temporal lobe – resection of the tip of temporal lobe, approx. 3 cm from the pole and resection of deep structures of the temporal lobe); MST method was performed to cut the pathways between the areas that could not be resected. This case shows a desired concordance of the presented mmp/LORETA source localization from interictal scalp EEG discharge areas of ictal discharges seen while performing ECoG.

Despite these promising results it should be stated that our methodology inherits the drawbacks of LORETA inverse solution, as discussed widely in the literature (Pascual-Marqui et al. 1994, Trujillo-Barreto et al. 2004). However it has been shown that the use of a proper time-frequency modeling of the EEG signals can lead to more robust results with the same inverse solution, showing reliable sources even in the absence of a heavy statistical postprocessing of the solutions (Konig et al. 2001).

These results also open different ways to improve performance of this kind of methods. First of all other implementations of multichannel matching pursuit can be used with different dictionaries and different choice of the best atom in each iteration. On the other hand, improvements from the inverse solution point of view can be also achieved, since it is well known that LORETA is really useful only in those cases in which wide areas of the cortex are strongly activated. Likewise, it is almost impossible to recover sources in deep areas such as thalamic and brainstem activations, which are usually reflected in more cortical (but non activated) areas like insulas for example. In this sense the use of other kind of

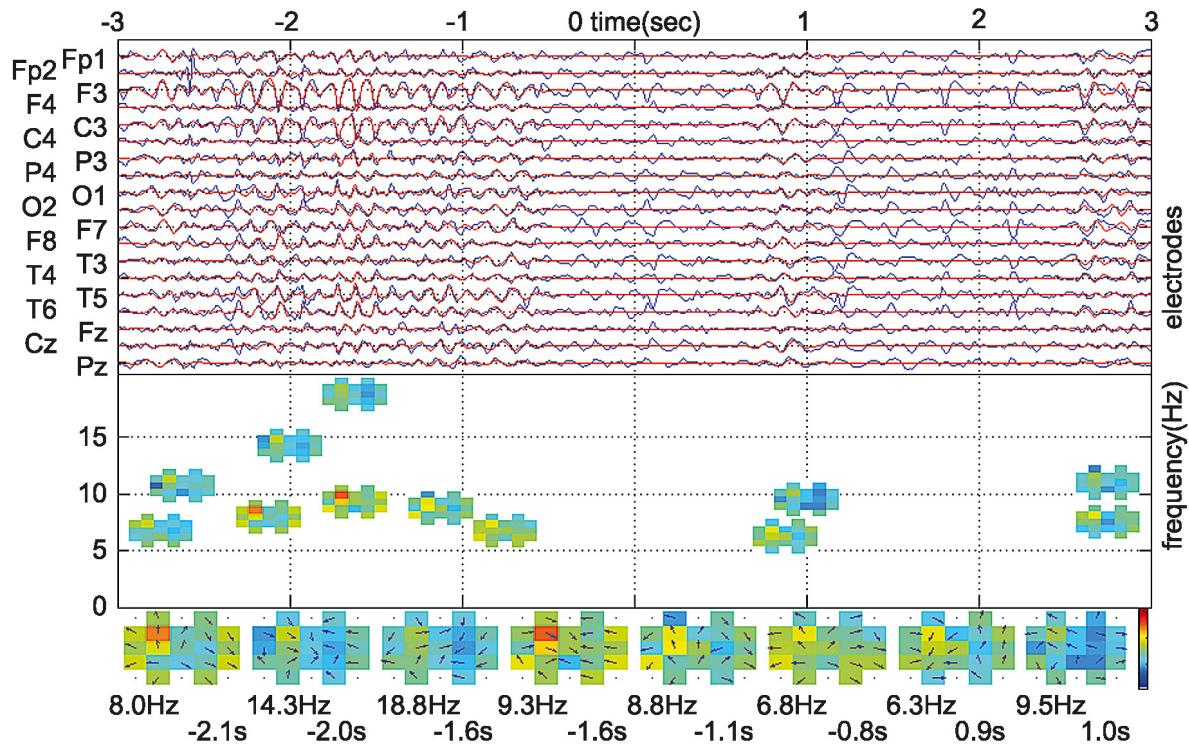


Fig. 4. Top: filtered EEG signal (blue) and real part of signal constructed from time-frequency atoms chosen as epileptic ones (red). Middle: schematic spatio-time-frequency map for chosen atoms. Bottom: schematic complex topographies (amplitudes denoted by colors, phases by arrows) for 8 time-frequency atoms (front of the head upwards).

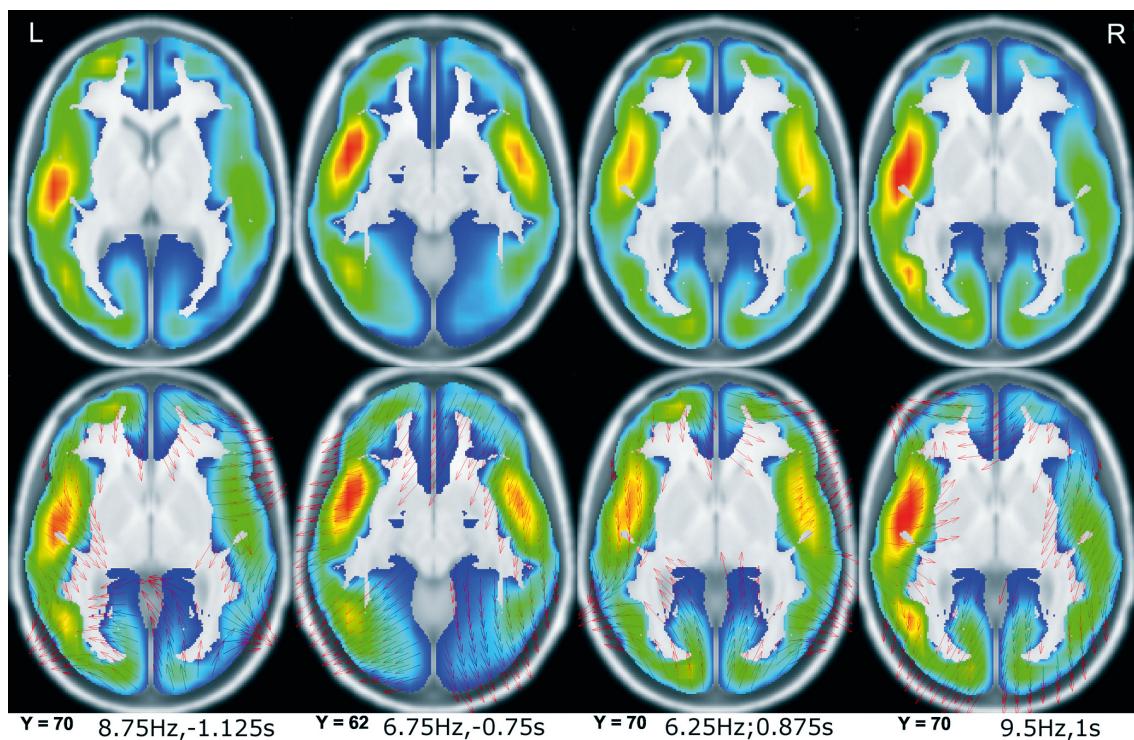


Fig. 5. Norm and normalized directions of the real part of PCD vectors for four time-frequency atoms from Fig. 4 (visualized in BetViewer, developed in Cuban Neuroscience Center, see Software section).

instantaneous inverse solutions based on Bayesian Theory (Trujillo-Barreto et al. 2004) can improve the localization task. Finally, within the same paradigm other EEG inverse solution methods can be used in place of LORETA.

## CONCLUSIONS

This work presents the application of a new methodology to the 3D localization of sources of epileptic activity in the brain, based on that introduced in Durka and coauthors (2005). Novelty of the proposed approach consists of using complex Gabor atoms. Its application to a case study demonstrated the desired correspondence between sources obtained by our methodology and those determined by ECoG in surgery. It also showed its ability of recognizing several mixed sources.

## REFERENCES

- Bracewell RN (1986) The Fourier transform and its applications. McGraw-Hill Book Company.
- Durka PJ, Matysiak A, Martinez Montes E, Valdes Sosa P, Blinowska KJ (2005) Multichannel matching pursuit and EEG inverse solutions. *J Neurosci Methods* 148: 49–59.
- Geva AB (1998) Biolectric sources estimation using spatio-temporal matching pursuit. *J Applied Signal Proc* 5: 195–208.
- Gribonval R (2003) Piecewise linear source separation. *Proceedings of the SPIE* 5207: 297–310.
- Holmes MD, Brown M, Tucker DM (2004) Are "generalized" seizures truly generalized? Evidence of localized mesial frontal and frontopolar discharges in absence. *Epilepsia* 45: 1568–1579.
- Konig T, Marti-Lopez F, Valdes-Sosa P (2001) Topographic time-frequency decomposition of the EEG. *Neuroimage* 14: 383–390.
- Mallat S, Zhang Z (1993) Matching pursuit with time-frequency dictionaries. *IEEE Transactions on Signal Processing* 41: 3397–3415.
- Martinez-Montes E, Valdes-Sosa P, Miwakeichi F, Goldman RI, Cohen MS (2004) Concurrent EEG/fMRI analysis by multi-way partial least squares. *Neuroimage* 22: 1023–1034.
- Martinez-Montes E, Bosch-Bayard J, Matysiak A, Durka P, Rodriguez-Puentes Y (2005) Adaptive time-frequency approximations vs. spectral integrals as preprocessing for EEG inverse solutions [abstract]. *Proceedings of the 11th Annual Meeting of the Organization for Human Brain Mapping* (available on CD-Rom in Neuroimage, Vol. 26, No.1).
- Miwakeichi F, Martinez-Montes E, Valdes-Sosa P, Nishiyama N, Hiroaki M, Yamaguchi Y (2004) Decomposing EEG data into space-time-frequency components using parallel factor analysis. *Neuroimage* 22: 1035–1045.
- Pascual-Marqui RD, Michel CM, Lehman D (1994) Low resolution electromagnetic tomography: A new method to localize electrical activity in the brain. *Int J Psychophysiol* 18: 49–65.
- Riera J, Fuentes ME (1997) Electric lead field for a piecewise homogeneous volume conductor model of the head. *IEEE Trans Biomed Eng* 45: 746–753.
- Tikhonov AN, Arsenin VY (1997) Solutions of Ill-Posed Problems. W.H. Winston, Washington DC.
- Trujillo-Barreto NJ, Aubert E, Valdes-Sosa PA (2004) Bayesian model averaging in EEG/MEG imaging. *Neuroimage* 21: 1300–1319.
- Worrell GA, Lagerlund TD, Sharbrough FW, Brinkmann BH, Busacker NE, Cicora KM, O'Brien TJ (2000) Localization of the epileptic focus by low-resolution electromagnetic tomography in patients with a lesion demonstrated by MRI. *Brain Topogr* 12: 273–82.

Received 1 July 2005, accepted 21 October 2005